32nd Symposium on Naval Hydrodynamics
Hamburg, Germany, 5-10 August 2018

Large eddy simulation of flow over axisymmetric hull

P. Kumar[1] and K. Mahesh[1]
([1]Department of Aerospace Engineering & Mechanics, University of Minnesota, USA)

ABSTRACT

Wall-resolved large-eddy simulation (LES) is performed for flow over the axisymmetric hull of DARPA SUBOFF without appendages at a Reynolds number $Re = 1.1 \times 10^6$, based on freestream velocity and the hull length. LES results show good agreement with the available experimental data and are used to describe the hull boundary layer in detail. The hull boundary layer evolves under streamwise varying pressure gradient. The axisymmetric turbulent boundary layer on the hull shows higher skin-friction and higher radial decay of turbulence away from the wall, compared to a planar turbulent boundary layer under similar conditions. The presence of transverse curvature decreases turbulent kinetic energy away from the wall, pointing to a possible suppression of the flow structures in the boundary layer at that location.

INTRODUCTION

The paper is focused on the flow over an axisymmetric hull of the generic submarine model, DARPA SUBOFF without appendages (AFF1) (Groves et al., 1989) as shown in Figure 1. The SUBOFF geometry, with and without appendages, has been used in numerous past experiments (Huang et al., 1992; Atsavapranee et al., 2004; Jiménez et al., 2010b,c) and simulations (Yang and Löhner, 2003; Alin et al., 2010; Vaz et al., 2010; Chase and Carrica, 2013; Chase et al., 2013; Posa and Balaras, 2016, 2018) employing a variety of numerical algorithms. The resolution requirement makes direct numerical simulations (DNS) of flow over hull geometries computationally intractable. Large eddy simulation approaches for simulating complex marine flows are becoming popular as they can provide more accurate results compared to Reynolds-averaged Navier–Stokes (RANS) based methods (Mahesh et al., 2015).

There are two main features of the flow field generated by flow over hull: hull boundary layer and wake. The wakes of both un-appended and fully-appended SUBOFF have been extensively described in past work. The hull boundary layer has received relatively less attention. Computationally, wall-resolved LES of flow over hull requires a fine near-wall resolution and a big domain to avoid confinement effects to capture near-wall structures that determine drag.

Figure 1: Geometry of axisymmetric hull of DARPA SUBOFF (AFF1) (Groves et al., 1989).

Posa and Balaras (2016) performed wall-resolved LES of a fully-appended SUBOFF at $Re = 1.2 \times 10^6$, based on the experiments of Jiménez et al. (2010c). They observed that the hull boundary layer was affected by the junction flows generated by the appendages. The hull boundary layer turns turbulent after tripping at $x/D = 0.25$ on the bow and grows from $Re_\theta \sim 1000$ at $x/L = 0.2$ to $Re_\theta \sim 2200$ at $x/L = 0.7$ on the hull. Posa and Balaras (2018) compared towed and self-propelled configurations of the SUBOFF and observed that the presence of the propeller significantly affects the hull boundary layer in the stern region but the mid-body region remains unaffected.

Kumar and Mahesh (2018b) performed LES of flow over the axisymmetric hull at $Re = 1.1 \times 10^6$, based on the experiments of Jiménez et al. (2010b). The LES results were compared to the available data showing good agreement and the evolution of the axisymmetric wake is discussed in detail. In the present study, we focus on the evolution of the turbulent boundary layer over the axisymmetric hull. Note that the hull boundary layer in the present study is purely axisymmetric unlike the experiments, where the presence of the semi-infinite sail as a support distorts the axisymmetry.

The rest of the paper is as follows. A brief overview of axisymmetric turbulent boundary layers (TBL) is provided, followed by a brief description of the numerical simulations and the computational setup. The simulation results for the hull boundary layer are compared to the available data and discussed. The paper concludes with a brief summary.

AXISYMMETRIC TURBULENT BOUNDARY LAYERS

The displacement thickness (δ^*) and the momentum thickness (θ) for axisymmetric boundary layers are defined (Luxton et al., 1984) such that,

$$(\delta^*+a)^2-a^2 = 2\int_a^{a+\delta}\left(1-\frac{U}{U_e}\right)rdr, \quad (1)$$

$$(\theta+a)^2-a^2 = 2\int_a^{a+\delta}\frac{U}{U_e}\left(1-\frac{U}{U_e}\right)rdr, \quad (2)$$

where a is the radius of curvature, U_e is the velocity at the edge of the boundary layer, i.e. $U_{a+\delta}=U_e$. Note that Eqs. (1, 2) reduce to the commonly known definitions of δ^* and θ for planar boundary layers as δ/a approaches zero.

A radius-based Reynolds number (Re_a) can be defined for an axisymmetric boundary layer such that $Re_a = aU/\nu$, where U is freestream velocity, ν is kinematic viscosity and a is the radius of cylinder. But Re_a does not include any effect of wall-shear stress or boundary layer thickness. Therefore, popular non-dimensional parameters to characterize axisymmetric TBL are the ratio of boundary layer thickness to the radius of curvature (δ/a) and the radius of curvature in wall units (a^+). Based on these two parameters, Piquet and Patel (1999) identified three regimes: (i) both δ/a and a^+ are large, (ii) large δ/a and small a^+ and (iii) small δ/a and large a^+. The first flow regime is observed for axial flow over a long slender cylinder at high *Re*, where a large effect of curvature is felt. The second flow regime is realized for axial flow over slender cylinders at low *Re*, where the axisymmetric TBL behaves like an axisymmetric wake with an inner layer with strong curvature and low-Re effects. Almost all the experimental studies reported in the literature have focused on the first two regimes (see Piquet and Patel, 1999). The third flow regime is common in applications where the Reynolds number is high but the boundary layer is thin compared to the radius of curvature. Usually, this flow regime is treated as a planar boundary layer where the curvature effects are assumed minimal. However, there are significant fundamental differences between a planar TBL and a thin axisymmetric TBL at high *Re*, such as increased skin-friction and rapid radial decay in turbulence away from the wall (Lueptow, 1990).

Axisymmetric TBL have not received the same attention as planar TBL likely due to the inherent difficulties in keeping the flow perfectly axial and prevent sagging or elastic deformation of the cylinders. The effect of curvature has been the focus of most past studies. Richmond (1957) and Yu (1958) conducted the first few experimental studies for curvature effects on boundary layers, which was followed by extensive experimental studies (Rao, 1967; Cebeci, 1970; Rao and Keshavan, 1972; Chase, 1972; Patel, 1974; Patel et al., 1974; Willmarth et al., 1976; Luxton et al., 1984; Lueptow et al., 1985; Krane et al., 2010) showing that the transverse curvature indeed has a significant effect on the overall behavior of axisymmetric TBL.

Afzal and Narasimha (1976) analyzed thin axisymmetric TBL at high *Re* (regime 3 described above) using asymptotic expansions and modified the well-known classical law of the wall for planar TBL to include the effect of curvature. The wall-normal distance in wall units (y^+) was modified as,

$$y^+ = a^+ ln(1+y/a) \quad (3)$$

where, $a^+ = au_\tau/\nu$ is the radius of curvature in wall-units. Using this modified y^+, it was shown that there exists a log layer in the mean velocity profile similar to that found in planar TBL, with the same slope but the intercept (B) is a weak function of curvature ($B = 5+236/a^+$). It has been shown that $U^+ = a^+ ln(1+y/a)$ is valid in the viscous sublayer region, but the use of y^+ from eq. 3 instead of the planar y^+ in the logarithmic region assumes that transverse curvature affects both the viscous sublayer and log layer identically.

One of the earliest numerical simulations of axisymmetric boundary layers were performed by Cebeci (1970), who showed higher skin-friction compared to planar prediction in both laminar and turbulent regimes. Similar behavior of skin-friction was observed in numerous subsequent simulations of axisymmetric TBL. Axisymmetric TBL over long thin cylinders have been extensively studied by Tutty (2008) using RANS and Jordan (2011, 2013, 2014a,b) using direct numerical simulations (DNS) and large eddy simulations (LES). Jordan used his simulation database to propose simple models for the skin-friction (Jordan, 2013) and the flow field (Jordan, 2014b). None of the studies mentioned so far have considered pressure gradient effects. Experiments by Fernholz and Warnack (1998) and Warnack and Fernholz (1998) considered axisymmetric TBL under favorable pressure gradient (FPG) in internal flow. Boundary layers under adverse pressure gradients (APG) have also been studied in the past using asymptotic expansions (See Afzal (1983, 2008) and the references therein).

SIMULATION DETAILS

Numerical method

In LES, large scales are directly accounted for by the spatially filtered Navier–Stokes equations, whereas the effect of small scales is modeled. The spatially filtered incompressible Navier–Stokes equations are formulated for the absolute velocity vector in the inertial frame as follows:

$$\begin{aligned} \frac{\partial \overline{u}_i}{\partial t} + \frac{\partial}{\partial x_j}(\overline{u}_i \overline{u}_j) &= -\frac{\partial \overline{p}}{\partial x_i} + \nu \frac{\partial^2 \overline{u}_i}{\partial x_j \partial x_j} - \frac{\partial \tau_{ij}}{\partial x_j}, \\ \frac{\partial \overline{u}_i}{\partial x_i} &= 0, \end{aligned} \tag{4}$$

where u_i is the velocity in the inertial frame, p is the pressure, ν is the kinematic viscosity, the overbar $\overline{(.)}$ denotes the spatial filter and $\tau_{ij} = \overline{u_i u_j} - \overline{u}_i \overline{u}_j$ is the sub-grid stress. The dynamic Smagorinsky model proposed by Germano et al. (1991) and modified by Lilly (1992) is used to model the subgrid stress terms. The Lagrangian time scale is dynamically computed based on surrogate–correlation of the Germano–identity error (Park and Mahesh, 2009). This approach extended to unstructured grids has shown good performance for a variety of flows including plane channel flow, circular cylinder and flow past a marine propeller in crashback (Verma and Mahesh, 2012).

Eq. (4) is solved by a numerical method developed by Mahesh et al. (2004) for incompressible flows on unstructured grids. The algorithm is derived to be robust without any numerical dissipation. It is a finite volume method where the Cartesian velocities and pressure are stored at the centroids of the cells and the face normal velocities are stored independently at the centroids of the faces. A predictor–corrector approach is used. The predicted velocities at the control volume centroids are first obtained and then interpolated to obtain the face normal velocities. The predicted face normal velocity is projected so that the continuity equation in Eq. (4) is discretely satisfied. This yields a Poisson equation for pressure which is solved iteratively using a multigrid approach. The pressure field is used to update the Cartesian control volume velocities using a least-square formulation. Time advancement is performed using an implicit Crank–Nicholson scheme. The algorithm has been validated for a variety of problems over a range of Reynolds numbers (see Mahesh et al., 2004). Chang et al. (2011) used this algorithm to perform wall-resolved LES of weakly separated flows on a range of Re. Recently, Kumar and Mahesh (2017) used this algorithm to accurately simulate complex propeller wakes and the results were used by Keller et al. (2018, 2017) to examine the acoustic field of the propeller.

Computational setup

LES of flow over hull is performed using a cylindrical computational domain of length $28.8D$ and diameter $12D$, where D is the maximum diameter of the hull. The origin of the reference coordinate system is located at the nose of the hull. The inflow plane is located $3D$ upstream of the hull whereas the outflow is located $17.2D$ downstream of the stern. Note that the length of the hull is $L = 8.6D$.

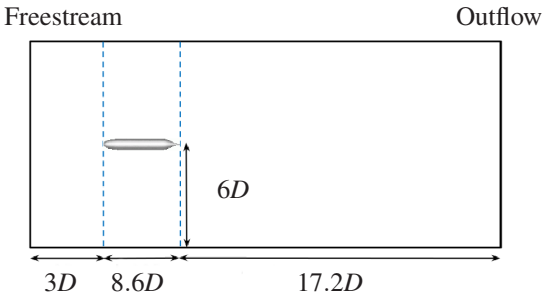

Figure 2: The computational domain used for simulations of flow over hull.

The physical conditions of the present simulations are identical to that of the experiments conducted by Jiménez et al. (2010b), with the difference that a semi-infinite sail was used as support in the experiments. The hull boundary layer in the simulations stays laminar in the absence of tripping. The hull boundary layer therefore is tripped at the same location $x/L = 0.087$ ($x/D = 0.75$) as that of the experiment, by applying a steady wall-normal velocity perturbation. This lifts the boundary layer and mimics the presence of a trip wire. This method of tripping was tested in preliminary simulations, where a small steady wall-normal velocity over few cells quickly turned an axisymmetric laminar boundary layer turbulent.

The computations are performed on an unstructured grid consisting of approximately 608 million hexahedral control volumes partitioned over 8192 processors. The computational time step $\Delta t U/D = 0.0006$ is used which corresponds to $\Delta t U/y_n = 2$, where y_n is the first wall-normal spacing near the hull. The simulations are performed for over two flow-through times to discard transients and the results are sampled for another two flow-through times to compute converged statistics. Freestream velocity boundary conditions are specified at the inflow and the lateral boundaries. Convective boundary conditions are prescribed at the outflow. No-slip boundary conditions are prescribed on the hull surface. A schematic of the computational domain and the boundary conditions is shown in figure 2. The reader is referred to Kumar and Mahesh (2018b) and Kumar (2018) for grid convergence studies and validation

with past experiments. LES results for the hull boundary layer is described in the next section.

HULL BOUNDARY LAYER

Pressure and skin-friction coefficients

Figure 3 shows the pressure (C_p) and skin-friction (C_f) coefficients on the hull, compared to the experimental data of Huang et al. (1992). The pressure and skin-friction coefficients are defined as:

$$C_p = \frac{p - p_\infty}{0.5\rho U_\infty^2} \quad \text{and} \quad C_f = \frac{\tau_w}{0.5\rho U_\infty^2}. \tag{5}$$

The reference pressure (p_∞) is taken at the inflow near the radial boundary, ρ is the density and U_∞ is the freestream velocity, and τ_w is the shear-stress at the wall.

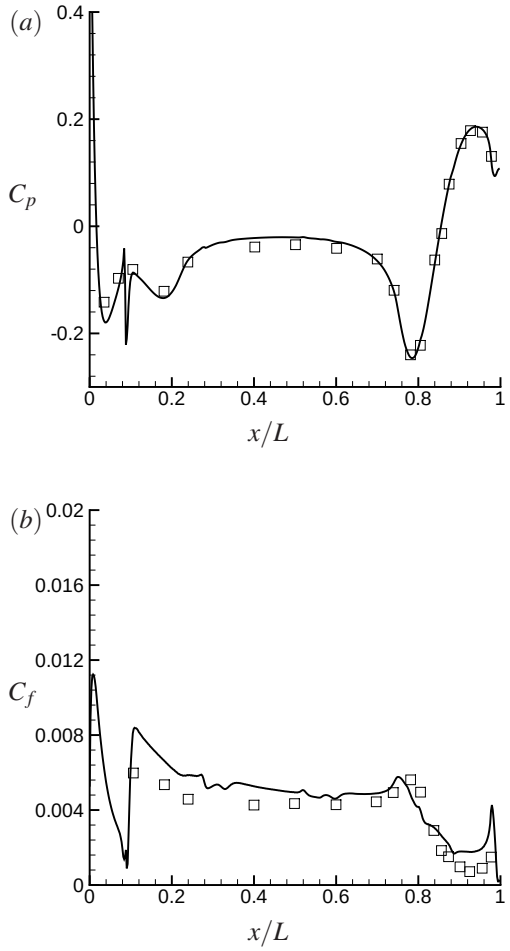

Figure 3: C_p (a) and C_f (b) on the hull compared to the experiments of Huang et al. (1992) at $Re = 1.2 \times 10^7$ shown by symbols. C_f from the experiments are scaled to the Re of the simulations using scaling law, $C_f \sim Re^{-0.2}$.

The experiments of Huang et al. (1992) were conducted at $Re = 1.2 \times 10^7$, whereas the present simulations are performed at $Re = 1.1 \times 10^6$. C_p is insensitive to Re for high Re attached flows but C_f depends on Re. Hence, C_f values of the experiments are scaled to the Re of the simulations using $C_f \sim Re^{-0.2}$ which applies to zero-pressure-gradient boundary layers (Schlichting, 1968). Note that the spike visible in the plots at $x/L = 0.087$ ($x/D = 0.75$) is due to tripping. The difference between the C_f from LES and the experiments on the bow and the stern regions is possibly due to inapplicability of the scaling law in regions of pressure gradient. The difference in C_f on the bow region can also be due to the difference in tripping with the experiments. Overall, LES results show good agreement with the experiments.

Mean flow field

The hull boundary layer turns turbulent after tripping on the bow and evolves under nominally zero pressure gradient on the mid portion of the hull. Figure 4 shows the profile of mean axial velocity in viscous units at a representative location ($x/L = 0.42$) on the hull. DNS results of a planar TBL at $Re_\theta = 1551$ (Jiménez et al., 2010a) are also shown for comparison. Although the boundary layer thickness is similar ($\delta^+ \sim 900$), the friction-velocity (u_τ) for the hull boundary layer is higher, which makes U^+ smaller compared to the planar TBL value at similar Re_θ. This is due to the presence of transverse curvature, as observed in past experiments (see Lueptow, 1990).

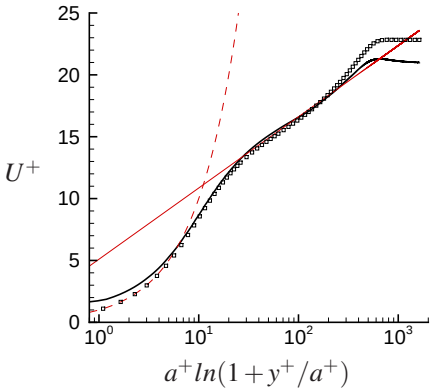

Figure 4: Profile of mean velocity in viscous units for the hull boundary layer at $x/L = 0.42$ on the hull is shown. Symbols show DNS of a planar TBL at $Re_\theta = 1551$ (Jiménez et al., 2010a).

In order to understand and quantify the effect of transverse curvature on axisymmetric boundary layers, Kumar and Mahesh (2018a) derived an analytical relation between C_f, pressure gradient and the boundary layer

integral quantities from the governing equations for an axisymmetric boundary layer evolving under streamwise pressure gradient as

$$C_f = \frac{2\left(1+\frac{\theta}{a}\right)\frac{d\delta^*}{dx}}{H+\beta_{RC}\left[2+H\left(1+\frac{\delta^*}{2a}+\frac{\theta^2}{a\delta^*}\right)\right]}, \qquad (6)$$

where $H = \delta^*/\theta$ is the shape-factor and β_{RC} is the Rotta–Clauser pressure gradient parameter Rotta (1953); Clauser (1954) defined as

$$\beta_{RC} = \frac{\delta^*}{u_\tau^2}\frac{1}{\rho}\frac{dP}{dx} = -\frac{\delta^*}{u_\tau^2}U_e\frac{dU_e}{dx}. \qquad (7)$$

The relation (Eq. 6) was shown to hold for a variety of axisymmetric boundary layers (see Kumar and Mahesh, 2018a) and was used to show that the presence of transverse curvature increases C_f if $\beta_{RC} \geq 0$ regardless of the value of a.

Profiles of root-mean-square (rms) of velocity fluctuations, Reynolds stress, rms of pressure fluctuations and the turbulent kinetic energy (TKE) are shown at the same location in Figure 5 (a-c). All the quantities are plotted in viscous units. Note that rms of radial (u_r) and azimuthal (u_θ) velocity fluctuations are shown for the hull boundary layer whereas rms of wall-normal (v) and spanwise (w) velocity are shown for the planar TBL (Jiménez et al., 2010a). In general, the profiles of second-order velocity (Figure 5a) statistics of the hull boundary layer show a similar trend as the planar TBL. However, the radial decay in velocity fluctuations away from the wall is faster compared to the planar TBL.

Figure 5 (b) shows rms of pressure fluctuations in viscous units along with the planar TBL. The difference between the two profiles are prominent, with the pressure fluctuations of the hull boundary layer decaying quicker than the planar TBL away from the wall. Note that $p^+_{rms} = p/(\rho u_\tau^2)$ where p is the pressure fluctuation. This implies that p^+_{rms} is more sensitive to the change in u_τ (C_f). The turbulent kinetic energy (TKE) profile of the hull boundary layer is compared to that of the planar TBL in Figure 5(c). The radial decay in TKE of the hull boundary layer is faster compared to the planar TBL. The curvature parameter is $\delta/a \approx 0.3$ at this location. It appears that curvature significantly affects the flow field in the logarithmic region of the boundary layer.

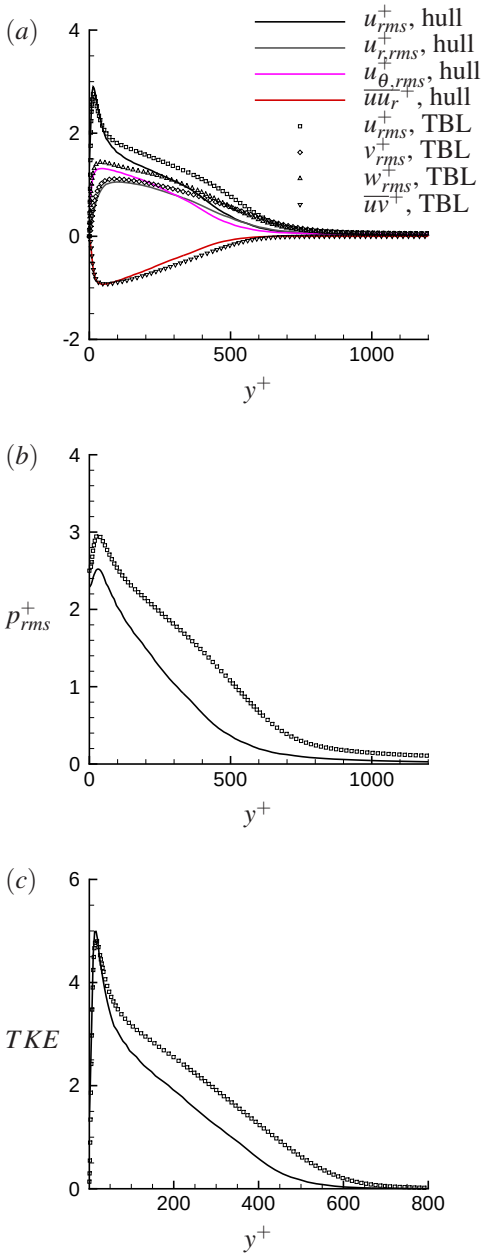

Figure 5: Second-order statistics in viscous units for the hull boundary layer at $x/L = 0.42$ on the hull are shown for rms of velocity fluctuations (u^+_{rms}, $u^+_{r,rms}$, $u^+_{\theta,rms}$), Reynolds stress ($\overline{uu_r}^+$) (a), rms of pressure fluctuations (p^+_{rms}) (b), and turbulent kinetic energy (c). Symbols show DNS of a planar TBL at $Re_\theta = 1551$ (Jiménez et al., 2010a).

Note that the profiles of rms of velocity and pressure fluctuations of the hull boundary layer show substantially different behavior in the logarithmic region compared to the planar TBL. For example, normalizing the profiles with identical u_τ, would not collapse the

profiles of the hull boundary layer on their planar counterpart. In order to have a closer look at the hull boundary layer, cylindrical planes parallel to the hull surface are extracted at two radial locations $r = 0.836$ and 0.862, which correspond to $y^+ = 10$ and 110 from the hull surface respectively, as shown in Figure 6 for instantaneous axial velocity and vorticity magnitude. The streaky flow structures in the buffer layer which are source of skin-friction (Kline et al., 1967), can be observed clearly in Figure 6(a) as marked by lower axial velocity. No such structures are observed in the logarithmic layer.

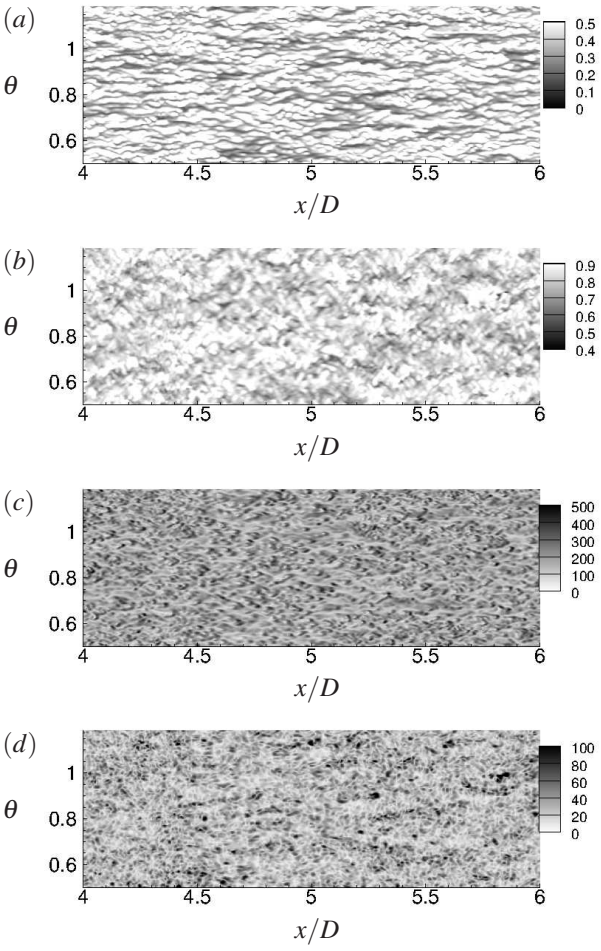

Figure 6: Instantaneous axial velocity (a,b) and vorticity magnitude (c,d) in the hull boundary layer at wall-parallel cylindrical planes at radial distance $r = 0.836$ (a,c) and 0.862 (b,d) from the axis, which correspond to approximate $y^+ = 10$ and 110 respectively away from the hull surface.

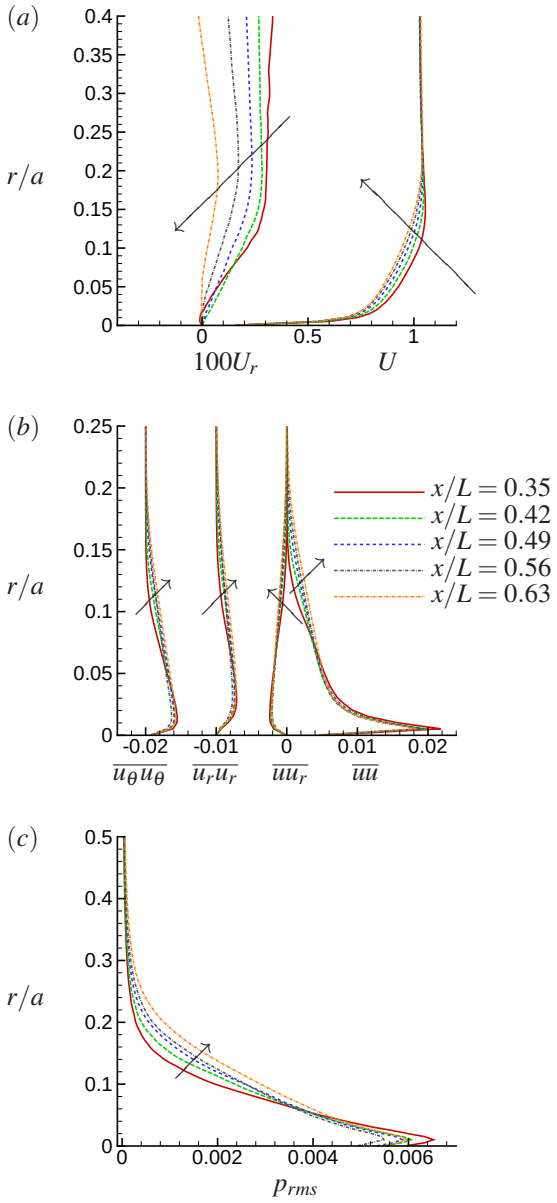

Figure 7: Profiles of mean velocity (U, U_r) (a), Reynolds stress components ($\overline{uu}$, $\overline{u_r u_r}$, $\overline{u_\theta u_\theta}$, $\overline{uu_r}$) (b), and rms of pressure fluctuations (p_{rms}) (c) are shown at five streamwise locations on the hull from $x/L = 0.35$ to 0.63. Note that the profiles of $\overline{u_r u_r}$ and $\overline{u_\theta u_\theta}$ are shifted to left by 0.01 and 0.02 units respectively for clarity. Arrows show the direction of increasing x.

The logarithmic layer region of turbulent boundary layers are known to be populated with the so-called *superstructures*, when *Re* is sufficiently large (Ganapathisubramani et al., 2003; Tomkins and Adrian, 2003). The experiments of Ganapathisubramani et al. (2003) were conducted on a TBL at $Re_\theta = 2500$ whereas

that of Tomkins and Adrian (2003) were conducted at $Re_\theta = 1015$ and 7705. The Re_θ of the hull boundary layer in the mid hull region is slightly lower compared to Ganapathisubramani et al. (2003). Note that the azimuthal resolution employed in the present simulations are adequate to resolve *superstructures*. At this point, the reason for the reduction in TKE in that region is not clear. It is conjectured that the presence of transverse curvature suppresses the flow structures in the logarithmic region of the TBL. This aspect of the axisymmetric TBL will be explored in future work.

The streamwise growth of the hull boundary layer is examined in Figure 7. Profiles of mean and second-order velocity statistics are shown at five streamwise locations on the hull ($0.35 \leq x/L \leq 0.63$) in Figures 7(a) and (b) respectively. The rms of pressure fluctuations at these locations are shown in Figure 7(c). The radius of curvature (a) at these locations are nearly constant. All the profiles are normalized using the freestream velocity. The spatial growth of the boundary layer thickness is clearly evident in all these plots. The second-order velocity statistics show streamwise variation only in the outer part of the boundary layer, whereas the rms of pressure fluctuations vary throughout the boundary layer. The peaks of the profiles of rms of pressure fluctuations are located at nearly the same radial location away from the wall.

SUMMARY AND FUTURE WORK

The evolution of the axisymmetric hull boundary layer is discussed for flow over the axisymmetric hull of DARPA SUBOFF without appendages at a Reynolds number $Re = 1.1 \times 10^6$, based on freestream velocity and the hull length. Results show that the hull boundary layer has higher skin-friction and higher radial decay of turbulence away from the wall, compared to a planar turbulent boundary layer under similar conditions. The effect of transverse curvature on axisymmetric boundary layers are discussed. The decrease in TKE in the logarithmic region of the hull boundary layer points to a possible suppression of flow structures in the boundary layer at that location. Future work will focus on understanding and quantifying the effects of transverse curvature on the flow structures of axisymmetric turbulent boundary layers.

ACKNOWLEDGEMENT

This work is supported by the United States Office of Naval Research (ONR) under ONR Grant N00014-14-1-0289 with Dr. Ki-Han Kim as technical monitor. The computations were made possible through the computing resources provided by the U.S. Army Engineer Research and Development Center (ERDC) in Vicksburg, Mississippi on the Cray XE6, Copper and Garnet of High Performance Computing Modernization program (HPCMP). This research partly used the computer time provided by the Innovative and Novel Computational Impact on Theory and Experiment (INCITE) program on the resources of the Argonne Leadership Computing Facility (ALCF), which is a DOE Office of Science User Facility supported under Contract DE-AC02-06CH11357. The authors thank Mr S. Anantharamu for his help with the grid pre-processing needed for the massively parallel computations reported in this paper.

REFERENCES

Afzal, N. "Analysis of a turbulent boundary layer subjected to a strong adverse pressure gradient". International Journal of Engineering Science, 21(6): 563–576, 1983.

Afzal, N. "Turbulent boundary layer with negligible wall stress". Journal of Fluids Engineering, 130(5):051205, 2008.

Afzal, N. and Narasimha, R. "Axisymmetric turbulent boundary layer along a circular cylinder at constant pressure". Journal of Fluid Mechanics, 74(01): 113–128, 1976.

Alin, N., Bensow, R. E., Fureby, C., Huuva, T., and Svennberg, U. "Current capabilities of DES and LES for submarines at straight course". Journal of Ship Research, 54(3):184–196, 2010.

Atsavapranee, P., Forlini, T., Furey, D., Hamilton, J., Percival, S., and Sung, C. H. "Experimental measurements for cfd validation of the flow about a submarine model (onr body-1)". In Proceedings of the 25th Symposium on Naval Hydrodynamics, St. John's, Canada, pages 8–13, 2004.

Cebeci, T. "Laminar and turbulent incompressible boundary layers on slender bodies of revolution in axial flow". Journal of Basic Engineering, 92:545–554, 1970.

Chang, P. A., Vargas, A., Lummer, D., Jiang, M., and Mahesh, K. "Fully-resolved LES of weakly separated flows". In 20th AIAA Computational Fluid Dynamics Conference. AIAA, 2011.

Chase, D. M. "Mean velocity profile of a thick turbulent boundary layer along a circular cylinder". AIAA Journal, 10(7):849–850, 1972.

Chase, N. and Carrica, P. M. "Submarine propeller computations and application to self-propulsion of DARPA Suboff". Ocean Engineering, 60:68–80, 2013.

Chase, N., Michael, T., and Carrica, P. M. "Overset simulation of a submarine and propeller in towed, self-propelled and maneuvering conditions". International Shipbuilding Progress, 60(1-4):171–205, 2013.

Clauser, F. H. "Turbulent boundary layers in adverse pressure gradients". Journal of the Aeronautical Sciences, 21(2):91–108, 1954.

Fernholz, H. H. and Warnack, D. "The effects of a favourable pressure gradient and of the Reynolds number on an incompressible axisymmetric turbulent boundary layer. Part 1. the turbulent boundary layer". Journal of Fluid Mechanics, 359:329–356, 1998.

Ganapathisubramani, B., Longmire, E. K., and Marusic, I. "Characteristics of vortex packets in turbulent boundary layers". Journal of Fluid Mechanics, 478: 35–46, 2003.

Germano, M., Piomelli, U., Moin, P., and Cabot, W. H. "A dynamic subgrid–scale eddy viscosity model". Physics of Fluids A, 3:7:1760, 1991.

Groves, N. C., Huang, T. T., and Chang, M. S. Geometric Characteristics of DARPA suboff models:(DTRC Model Nos. 5470 and 5471). David Taylor Research Center, 1989.

Huang, T., Liu, H. L., Grooves, N., Forlini, T., Blanton, J., and Gowing, S. "Measurements of flows over an axisymmetric body with various appendages in a wind tunnel: the DARPA SUBOFF experimental program". In Proceedings of the 19th Symposium on Naval Hydrodynamics, 1992.

Jiménez, J., Hoyas, S., Simens, M. P., and Mizuno, Y. "Turbulent boundary layers and channels at moderate Reynolds numbers". Journal of Fluid Mechanics, 657: 335–360, 2010a.

Jiménez, J. M., Hultmark, M., and Smits, A. J. "The intermediate wake of a body of revolution at high Reynolds numbers". Journal of Fluid Mechanics, 659: 516–539, 2010b.

Jiménez, J. M., Reynolds, R. T., and Smits, A. J. "The effects of fins on the intermediate wake of a submarine model". Journal of Fluids Engineering, 132(3):031102, 2010c.

Jordan, S. A. "Axisymmetric turbulent statistics of long slender circular cylinders". Physics of Fluids (1994-present), 23(7):075105, 2011.

Jordan, S. A. "A skin friction model for axisymmetric turbulent boundary layers along long thin circular cylinders". Physics of Fluids (1994-present), 25(7): 075104, 2013.

Jordan, S. A. "On the axisymmetric turbulent boundary layer growth along long thin circular cylinders". Journal of Fluids Engineering, 136(5):051202, 2014a.

Jordan, S. A. "A simple model of axisymmetric turbulent boundary layers along long thin circular cylinders". Physics of Fluids (1994-present), 26(8):085110, 2014b.

Keller, J., Kumar, P., and Mahesh, K. "Large eddy simulation of propeller in forward mode of operation". In Fifth International Symposium on Marine Propulsors, Espoo, Finland, 2017.

Keller, J., Kumar, P., and Mahesh, K. "Examination of propeller sound production using large eddy simulation". Physical Review Fluids, 3(6):064601, 2018.

Kline, S. J., Reynolds, W. C., Schraub, F. A., and Runstadler, P. W. "The structure of turbulent boundary layers". Journal of Fluid Mechanics, 30(04):741–773, 1967.

Krane, M. H., Grega, L. M., and Wei, T. "Measurements in the near-wall region of a boundary layer over a wall with large transverse curvature". Journal of Fluid Mechanics, 664:33–50, 2010.

Kumar, P. Large Eddy Simulation of complex flow over submerged bodies. PhD thesis, University of Minnesota, USA, 2018.

Kumar, P. and Mahesh, K. "Large eddy simulation of propeller wake instabilities". Journal of Fluid Mechanics, 814:361–396, 2017.

Kumar, P. and Mahesh, K. "Analysis of axisymmetric boundary layers". Journal of Fluid Mechanics, 849: 927–941, 2018a.

Kumar, P. and Mahesh, K. "Large-eddy simulation of flow over an axisymmetric body of revolution". Journal of Fluid Mechanics, 853:537–563, 2018b.

Lilly, D. K. "A proposed modification of the Germano subgrid–scale closure model". Physics of Fluids A, 4:3: 633, 1992.

Lueptow, R. M. "Turbulent boundary layer on a cylinder in axial flow". AIAA Journal, 28(10):1705–1706, 1990.

Lueptow, R. M., Leehey, P., and Stellinger, T. "The thick, turbulent boundary layer on a cylinder: Mean and fluctuating velocities". Physics of Fluids (1958-1988), 28(12):3495–3505, 1985.

Luxton, R. E., Bull, M. K., and Rajagopalan, S. "The thick turbulent boundary layer on a long fine cylinder in axial flow". Aeronautical Journal, 88:186–199, 1984.

Mahesh, K., Constantinescu, G., and Moin, P. "A numerical method for large–eddy simulation in complex geometries". Journal of Computational Physics, 197:1:215, 2004.

Mahesh, K., Kumar, P., Gnanaskandan, A., and Nitzkorski, Z. "LES applied to ship research". Journal of Ship Research, 59(4):238–245, 2015.

Park, N. and Mahesh, K. "Reduction of the Germano-identity error in the dynamic Smagorinsky model". Physics of Fluids (1994-present), 21(6): 065106, 2009.

Patel, V. C. "A simple integral method for the calculation of thick axisymmetric turbulent boundary layers". The Aeronautical Quarterly, 25(1):47–58, 1974.

Patel, V. C., Nakayama, A., and Damian, R. "Measurements in the thick axisymmetric turbulent boundary layer near the tail of a body of revolution". Journal of Fluid Mechanics, 63(2):345–367, 1974.

Piquet, J. and Patel, V. C. "Transverse curvature effects in turbulent boundary layer". Progress in Aerospace Sciences, 35(7):661–672, 1999.

Posa, A. and Balaras, E. "A numerical investigation of the wake of an axisymmetric body with appendages". Journal of Fluid Mechanics, 792:470–498, 2016.

Posa, A. and Balaras, E. "Large-eddy simulations of a notional submarine in towed and self-propelled configurations". Computers & Fluids, 165:116–126, 2018.

Rao, G. N. V. "The law of the wall in a thick axi-symmetric turbulent boundary layer". Journal of Applied Mechanics, 89:237–338, 1967.

Rao, G. N. V. and Keshavan, N. R. "Axisymmetric turbulent boundary layers in zero pressure-gradient flows". Journal of Applied Mechanics, 39(1):25–32, 1972.

Richmond, R. L. Experimental Investigation of Thick, Axially Symmetric Boundary Layers on Cylinders at Subsonic and Hypersonic Speeds. PhD thesis, California Institute of Technology, 1957.

Rotta, J. "On the theory of the turbulent boundary layer". NACA Technical Memorandum, No. 1344, 1953.

Schlichting, H. Boundary-layer theory. McGraw-Hill, 1968.

Tomkins, C. D. and Adrian, R. J. "Spanwise structure and scale growth in turbulent boundary layers". Journal of Fluid Mechanics, 490:37–74, 2003.

Tutty, O. R. "Flow along a long thin cylinder". Journal of Fluid Mechanics, 602:1–37, 2008.

Vaz, G., Toxopeus, S., and Holmes, S. "Calculation of manoeuvring forces on submarines using two viscous-flow solvers". In Proceedings of the 29th International Conference on Ocean, Offshore and Arctic Engineering, Shanghai, China, 2010.

Verma, A. and Mahesh, K. "A Lagrangian subgrid-scale model with dynamic estimation of Lagrangian time scale for large eddy simulation of complex flows". Physics of Fluids (1994-present), 24(8):085101, 2012.

Warnack, D. and Fernholz, H. H. "The effects of a favourable pressure gradient and of the Reynolds number on an incompressible axisymmetric turbulent boundary layer. Part 2. the boundary layer with relaminarization". Journal of Fluid Mechanics, 359: 357–381, 1998.

Willmarth, W. W., Winkel, R. E., Sharma, L. K., and Bogar, T. J. "Axially symmetric turbulent boundary layers on cylinders: Mean velocity profiles and wall pressure fluctuations". Journal of Fluid Mechanics, 76 (01):35–64, 1976.

Yang, C. and Löhner, R. "Prediction of flows over an axisymmetric body with appendages". In The 8th International Conference on Numerical Ship Hydrodynamics, Busan, Korea, 2003.

Yu, Y. S. "Effects of transverse curvature on turbulent boundary layer characteristics". Journal of Ship Research, 3:33–41, 1958.

DISCUSSION

Michael Mattson,
CSRA Inc.

The authors should be complimented for an interesting paper detailing the nature of boundary layer turbulence on an axisymmetric hull.

1. How well does the analytical expression for the skin friction coefficient (Eqn. 6) compare against your measured results (Figure 3)?

2. Given that the turbulent kinetic energy (TKE) is reduced for the hull boundary layer as compared to a planar boundary layer, how does this affect the kinetic energy spectra? The low axial velocity structures are suppressed in the log layer (Figure 6), is it primarily the energy of the large structures that are reduced or is the suppression of TKE spread across all wavenumbers?

AUTHOR'S REPLY

Thank you for your comments and questions which are addressed below.

1. The skin friction coefficient expression is exact. However, it requires boundary layer integral parameters which were not provided in the measured data. Hence, we did not make any such comparison.

2. The discussion of the curvature effects on the kinetic energy spectra is interesting and we plan to address this by performing DNS of axisymmetric turbulent boundary layer in future studies.

DISCUSSION

Vladimir Serebryakov,
Institute of Hydromechanics of NASU.

1. Can you estimate influence of walls of channel on the hull surface under such conditions?

2. Considering hulls frequently are slender enough, can you apply equations of Slender Body Hydrodynamics here?

AUTHOR'S REPLY

Thank you for your comments and questions which are addressed below.

1. The influence of walls of channel on the hull surface can be estimated by reporting confinement effects, one measure of which is the ratio of crossectional area of the hull model to the tunnel crossection. We have performed detailed confinement studies (see the literature cited in the text) to ensure minimal effects of the far field boundaries.

2. One of the goals of the present work was to demonstrate the predictive capability of LES for such flows. We have therefore not considered the use of Slender Body Hydrodynamics.

DISCUSSION

Harald Svensson,
Saab Dynamics.

1. In connection to the over 8000 cores and grid size of the model it would be of value to include the CPU or clock time for a typical simulation to an acceptable degree of convergence.

AUTHOR'S REPLY

Thank you for your comment. The present simulation using 8192 cores took around 200 hours to get converged results.